Title
Live Imaging of Mouse Secondary Palate Fusion.

Authors
Kim, Seungil
Prochazka, Jan
Bush, Jeffrey O

Publication Date
2017

DOI
10.3791/56041

Peer reviewed

Video Article

Live Imaging of Mouse Secondary Palate Fusion

Seungil Kim[1], Jan Prochazka[2], Jeffrey O. Bush[1]

[1]Department of Cell and Tissue Biology, Program in Craniofacial Biology and Institute for Human Genetics, University of California San Francisco

[2]Laboratory of Transgenic Models Diseases, Czech Centre for Phenogenomics, Institute of Molecular Genetics of the Czech Academy of Sciences

Correspondence to: Jeffrey O. Bush at Jeffrey.bush@ucsf.edu

URL: https://www.jove.com/video/56041
DOI: doi:10.3791/56041

Keywords: Developmental Biology, Issue 125, live imaging, secondary palate, tissue fusion, cleft, craniofacial

Date Published: 7/27/2017

Citation: Kim, S., Prochazka, J., Bush, J.O. Live Imaging of Mouse Secondary Palate Fusion. *J. Vis. Exp.* (125), e56041, doi:10.3791/56041 (2017).

Abstract

The fusion of the secondary palatal shelves to form the intact secondary palate is a key process in mammalian development and its disruption can lead to cleft secondary palate, a common congenital anomaly in humans. Secondary palate fusion has been extensively studied leading to several proposed cellular mechanisms that may mediate this process. However, these studies have been mostly performed on fixed embryonic tissues at progressive timepoints during development or in fixed explant cultures analyzed at static timepoints. Static analysis is limited for the analysis of dynamic morphogenetic processes such a palate fusion and what types of dynamic cellular behaviors mediate palatal fusion is incompletely understood. Here we describe a protocol for live imaging of *ex vivo* secondary palate fusion in mouse embryos. To examine cellular behaviors of palate fusion, epithelial-specific *Keratin14*-cre was used to label palate epithelial cells in *ROSA26-mTmG*^{flox} reporter embryos. To visualize filamentous actin, *Lifeact-mRFPruby* reporter mice were used. Live imaging of secondary palate fusion was performed by dissecting recently-adhered secondary palatal shelves of embryonic day (E) 14.5 stage embryos and culturing in agarose-containing media on a glass bottom dish to enable imaging with an inverted confocal microscope. Using this method, we have detected a variety of novel cellular behaviors during secondary palate fusion. An appreciation of how distinct cell behaviors are coordinated in space and time greatly contributes to our understanding of this dynamic morphogenetic process. This protocol can be applied to mutant mouse lines, or cultures treated with pharmacological inhibitors to further advance understanding of how secondary palate fusion is controlled.

Video Link

The video component of this article can be found at https://www.jove.com/video/56041/

Introduction

Tissue fusion is an important step in the development of multiple organs. Major human birth defects such as cleft lip and palate, spina bifida and malformations of the heart can result from defects in tissue fusion[1]. Mouse secondary palate fusion has been extensively studied to identify the cellular and molecular mechanisms controlling tissue fusion in development[2,3,4]. In the mouse, secondary palate development starts at around E11.5 with the outgrowth of a secondary palatal shelf from each of the bilateral maxillary processes. Initial growth of the palatal shelves occurs vertically along the tongue, until approximately E14.0, at which time, the palatal shelves become elevated horizontally above the tongue. Medially-directed growth results in physical contact between the apposing epithelia of the two palatal shelves, forming the midline epithelial seam (MES) at E14.5. The intervening MES must be removed from between the secondary palatal shelves to allow mesenchymal confluence and the development of an intact, completely fused secondary palate by E15.5[3].

How a shared epithelial MES cell layer is formed between two separate palatal shelves, and then removed to achieve mesenchymal confluency, has been a central question in palate development. Based on mouse histological and electron microscopy (EM) studies, explant culture studies, and functional mouse genetics experiments, several fundamental cell behaviors have been implicated in this process. Filopodia-like projections from the medial edge epithelium MEE of each palatal shelf facilitates initial contact[5,6], followed by intercalation of these epithelial cells to a shared single MES[6,7]. Removal of the resulting shared MES has been proposed to proceed by three non-exclusive mechanisms. Early studies employing histological observation and *ex vivo* lineage tracing with vital dyes indicated that the MES might be removed by epithelial to mesenchymal transition (EMT) of MES cells[8,9], though more recently, genetic lineage tracing of epithelial cells has raised uncertainty as to the long-term contribution of epithelial cells to the palatal shelf mesenchyme[10,11,12]. Significant numbers of apoptotic cells, and a reduction in their number in some mutants that fail to undergo proper palate fusion has led to the idea that apoptosis may be a major driver of MES dissolution[2,3]. Finally, based initially on studies involving epithelial labeling and static observation at progressive timepoints, MES cells were proposed to migrate in the oronasal and anteroposterior dimensions[11,13], but such dynamic cell behaviors were initially unconfirmed due to an inability to observe them in live palatal tissue. Recently, we were able to directly observe these behaviors by developing a new live imaging methodology that combines mouse genetic methods of fluorescent labeling with confocal live imaging of explanted palatal shelves.

First, to visualize dynamic cellular behaviors in palate epithelial cells during palate fusion, we generated an epithelial-specific reporter mouse by crossing *ROSA26-mTmG*^{flox} mice with *Keratin14-cre* mice[14,15]. Confocal live imaging of palate explant culture of the resulting embryos confirmed some previously proposed cellular behaviors and identified novel events in the fusion process[6]. Epithelial cell membrane protrusions preceded initial cell-cell contact followed by epithelial convergence by cell intercalation and oronasal cell displacement. Notably, we also discovered that cell extrusion, a process reported to play important roles in epithelial homeostasis, was a major mechanism driving mouse secondary palate

fusion[6,16]. This imaging method can be used with other reporter lines; we utilized *Lifeact-mRFPruby* transgenic mice[17,18] to examine actin cytoskeletal dynamics during the fusion process. Other reporters can also be employed to observe other specific aspects of palate fusion and this method can be adapted either to laser scanning confocal microscopy or spinning disk confocal microscopy, depending on imaging needs and microscope availability. Live imaging is increasingly becoming a keystone approach in developmental biology. Particularly, craniofacial morphogenesis is complex and human birth defects that affect the face are common. This confocal live imaging method will help to enable an improved understanding of underlying basic developmental mechanisms as well as origins of human craniofacial abnormalities.

Protocol

All animal experiments were performed in accordance with the protocols of the University of California at San Francisco Institutional Animal Care and Use Committee.

1. Preparation of Live Imaging Media

1. **Preparation of liquid culture media**
    1. Add 20% fetal bovine serum (FBS), 2 mM L-glutamine, 100 U/mL penicillin, 100 µg/mL streptomycin, 200 µg/mL L-ascorbic acid, 15 mM HEPES to Dulbecco's Modified Eagle Medium (DMEM)/F12 media.
    NOTE: Live imaging media was freshly made right before the imaging. This media contains phenol-red which may lead to phototoxicity over long time courses of live imaging. Substituting for media without phenol-red may improve long-term imaging.

2. **Preparation of low melting agarose solution**
    1. Dissolve 350 mg of low-melting agarose in 10 mL of autoclaved distilled water to make a 3.5% stock solution.
    2. Mix the agarose solution well and incubate at 70 °C in a water bath to dissolve the agarose completely.
    3. Cool down the agarose solution in a 37 °C water bath before adding it to the live imaging media.
    4. Add 1 mL of the agarose stock solution to 5 mL of the liquid live imaging media to make a final concentration (0.6%).
    5. Keep the media with agarose in a 37 °C water bath to prevent premature solidification.

2. Preparation of Palate Explant Culture for Live Imaging

1. **Dissection of recently-adhered E14.5 secondary palatal shelves**
NOTE: In our experience imaging fusion requires starting with a slightly adhered pair of palatal shelves; this adherence prevents explant movements that prevent fusion from occurring during imaging.
    1. Dissect E14.5 stage embryos in 1x phosphate-buffered saline (PBS) and choose green fluorescent protein (GFP)-expressing (from *K14-cre; ROSA26-mTmG^{flox}*) or (Red fluorescent protein) RFP-expressing (from *Lifeact-mRFPruby*) positive embryos using a dissecting microscope equipped with fluorescent lamps. Transfer tissue to pre-warmed live imaging culture media without agarose.
    2. Cut the embryo head and remove upper brain area by using two fine No. 5 forceps (**Figure 1A-C**). Use one No. 5 forceps to hold the embryo while the other No. 5 forceps to cut away extra tissue outside the palatal shelves.
    NOTE: Fine scissors can be used to cut embryo head (the first step) instead of one No. 5 forceps. However, two No. 5 fine forceps will give better control to make precise cuts.
    3. Remove mandible carefully without damaging palatal shelves as shown in **Figure 1D** and **1E**. To reduce the chance of damaging palates, keep the tongue through dissection of the mandible, followed by careful removal of the tongue.
    4. After removing the mandible and tongue, examine the oral side of the secondary palate with a stereomicroscope with fluorescence to confirm strong reporter signal in the MES (**Figure 1M**).
    5. Dissect out posterior parts including hindbrain and brain stem after removing mandible and tongue (**Figure 1F**).
    6. Remove both maxillae with adhered palatal shelves (**Figure 1G**).
    7. Cut the anterior upper jaw tissue keeping both primary and secondary palate intact (**Figure 1H** and **I**).
    8. Remove nasal septum on nasal side of explant exposing the MES.
    NOTE: These later steps of dissections need careful attention not to disrupt the contacts between two secondary palatal shelves. Removal of the nasal septum helps to reduce background signal from other areas and also reduce vertical tissue movement, allowing stable imaging (**Figure 1J-L**).
    9. After dissecting the palatal shelves, examine the midline reporter signal again to make sure that there is no damage to the epithelial layer between the tissues.

2. **Setting up palate explants in culture dish with live imaging media**
    1. Put live imaging media into 35-mm glass bottom dish.
    2. Put dissected palatal shelves oral side facing down as close to the glass bottom as possible for imaging with an inverted confocal microscope (**Figure 1N**).
    3. Place dry ice pellets on a conductive surface nearby to the culture dish to expedite agarose solidification by decreasing temperature fast or put the culture dish at 4 °C. A cold plate, such as one used for paraffin embedding could also be used at this stage.
    NOTE: When dry ice is used, agarose media change needs to be monitored carefully to prevent freezing media.

3. Confocal Time-lapse Imaging of Palate Explant

1. **Imaging and Data acquisition**
    1. After agarose was semi-solidified, mount the culture dish in an inverted confocal microscope equipped with 37 °C incubation chamber. Use a white light confocal microscope and cell observer spinning disk confocal microscope.

NOTE: We used a modified media containing 15 mM HEPES without CO^2 gas.
2. Put petroleum jelly between the culture dish and cover using a syringe to prevent evaporation of media (**Figure 1N**).
   NOTE: Some condensation on top of the culture dish cover after overnight (O/N) culture occurs but the volume of media does not change suggesting that the petroleum jelly prevents media from evaporating.
3. Locate the region of interest with low magnification objectives (10x) and use higher magnification objectives (20x objective with 3x digital zoom or a 40x objective with Immersol W) for time-lapse live imaging.
   NOTE: Dissected secondary palatal shelves are not flat. The secondary palate is a curved structure and this makes it difficult to image the entire MES in the same plane. Low magnification (10x) imaging can allow whole palate imaging but 40x objectives will provide better image resolution to examine detailed cellular movements in deeper Z positions. The curvature is high in the middle palate region. Anterior and posterior palate are relatively flat compared to the middle palate. We often image toward the mid-anterior of the secondary palate to avoid regions of greatest curvature.
4. Scan multiple Z stacks with 5 µm each step for 16-24 h using proper laser excitation (488 nm for GFP and 532/561 nm for RFP) (**Figure 2**).
   NOTE: To reduce potential phototoxicity, use minimum laser power and exposure time. This is important especially in case of multi-color imaging. Use 22% of 552 nm laser power for membraneTomato (mT), 30% of 495 nm laser power for membraneGFP (mG) and 25% of 561 nm laser power for membraneRFP. Average exposure time was 550 ms.
5. Use image analysis software to perform cell tracking and quantitative analysis.

4. Data Image Analysis

NOTE: Here, Imaris was used. Similar data analyses may also be performed with ImageJ or Volocity software packages.

1. **Rendering 3-dimensional (3D) surfaces from image sequences.**
   NOTE: This section enables the generation of a surface from a movie generated with a membrane GFP signal.
   1. Click *Edit* | *Show Display Adjustment* and use the histogram slider to adjust the signal intensity so that the membrane signal is clear throughout the length of the movie (**Figure 3A**).
   2. Correct bleached signal by using Image *Processing* | *Attenuation Correction*. Adjust the Intensity Front and Intensity Back values so that the membrane signal is clear throughout the length of the movie. Some trial and error might be required in setting these values.
      NOTE: The Intensity Back (Deeper Z position) value will be less than the Intensity Front (Surface Z position) value due to limited laser penetration. These values can therefore also be changed to normalize signal intensity in the Z series. Both values may be adjusted to achieve bleaching correction. Attenuation correction is also called Emission attenuation correction[19].
   3. In order to generate a surface from the membrane signal, select *Surpass* | *Surfaces*, choose a source channel and Threshold type (Absolute Intensity) and under the Algorithm Settings select *Segment only a Region of Interest* and *Process of entire image finally*, followed by clicking on the forward arrow; continue to push the forward arrow (use default settings, or specify Surface Area Detail Levels and Thresholding method by trial and error), checking whether the generated surface reflects the fluorescence signal. To specify a Region of Interest, select region and time(s) to be rendered by cropping X, Y, Z positions.
      NOTE: Select *Process of entire image finally* so that adjustments and thresholds will be applied across the entire movie.
   4. Generate a surface by clicking the forward arrow button again. Then adjust the threshold by changing the histogram in *Filters* to correspond to the membrane signal.
   5. After the surface is generated, choose surface in Surfaces/Settings to visualize the surface signal and finish the surface generation process by pushing the double forward arrow button (**Figure 3B**).
   6. Go to *Surface* | *Edit* and click *Mask all* in the *Mask Properties* to generate a masked channel image.
   7. After clicking ok, the Mask Channel window will automatically open; select the GFP channel, set voxels outside the surface to the maximum signal intensity value (found in *Edit* | *Display adjustment*) and voxels inside the surface to the minimum GFP intensity value (also found in *Edit* | *Display adjustment*), in *Mask Settings* to generate a mask of the membrane signal.
   8. As the mask of the membrane signal will be shown in *Volume* view, generate inverted images by using *Image Processing* | *Contrast Change* | *Invert* (**Figure 3C**).

2. Detecting spots from inverted surface images.
   NOTE: This section allows the center of each cell to be marked with a unique spot and tracked over space and time.
   1. Select *Surpass Scene* | *Spots* | *Create*; in Algorithm Settings choose *Segment only a Region of Interest*, *Process of entire image finally* and *Track Spots (over time)*.
   2. Click on the forward arrow and specify a Region of Interest; select the region and time(s) to track spots; continue to push the forward arrow, choose the masked channel as a source channel and determine estimated XY diameter of spots.
   3. As clicking the forward arrow button will automatically open a filter window; adjust the spot detection threshold by changing values in the histogram to generate single spots at the center of each cell (**Figure 3D**).
   4. As clicking the forward arrow button again will open the *Algorithm* window., choose *Autoregressive motion tracking model*[20] and specify the maximum tracking distance and maximum gap size to connect tracks that become discontinuous for a short period of time.
   5. As clicking the forward arrow button again will open the Filters window, set the track duration threshold by adjusting the histogram so that every cell is tracked. Clicking the double forward arrow button will finalize spot detection.
   6. In order to correct tissue drift, click *Spots* | *Track Editor* and select *Correct Drift*. An *Algorithm* window will open automatically; select the select *Translational drift, Include entire result*, and *Correct objects positions*.

3. **Generating vantage plots for quantitative analysis.**
   NOTE: The program's Scatterplot is a tool to generate multi-dimensional (X, Y, Z, Color and Scale) graphs with multiple objects. These plots are useful for viewing trends of many cell movements over time.
   1. Make 2D or 3D plots of cell tracking data using the *Vantage-Add New Vantage* plot menu (**Figure 3E** and **3F**).
   2. Select *Volume* or *Spots* and Choose *Create/ Category* and *Plot Type*
   3. Adjust *Plot Values* to generate different Vantage graphs.

4. Export graphs using the *Snapshot* function.
   NOTE: Statistical data can also be exported as a spreadsheet for further quantitative analysis by clicking *Plot Numbers Area* | *Save*.

Representative Results

Live imaging of palate explant culture revealed multiple cellular processes mediating palate fusion[6]. Initial contacts between two epithelial cells are made by membrane protrusions (**Figure 2B-2E**). When two epithelial layers meet, they form a multi-cell layered MES followed by intercalation to make an integrated single cell-layer MES through epithelial convergence(**Figure 2A-2E** and **Figure 2K-2O**). Epithelial cells in deeper Z levels are also progressively displaced to the oral side of the MES contributing to the epithelial convergence process (**Figure 2K**). Posterior-directed cell migration was observed in middle palate MES (**Figure 2F-2J**). In addition, we found epithelial cell extrusion events during palate fusion suggesting that epithelial cells in the MES can be removed by this active process (**Figure 2Q, 2T**). The integrated epithelial seam will ultimately break down to achieve mesenchymal confluency (**Figure 2S, 2T**).

Lifeact-mRFPruby palate showed dynamic actin cytoskeletal rearrangements during palate fusion[6]. Filamentous actin became enriched at the border between epithelial and mesenchymal areas forming a cable-like structure along the anterior-posterior axis (**Figure 2K-2T)**. Actomyosin contractility drives epithelial convergence and MES breakage because chemical inhibition of either myosin activity or actin polymerization blocked these dynamic processes[6].

Software was used to trace cellular behaviors during palate fusion. The best method for cell tracking depends on the reporter signal. If a nuclear reporter mouse is used, the program can trace the center of fluorescent signals as cellular centers[21]. Nuclear GFP reporter mouse such as *ROSA26*$^{GFP\text{-}NLS\text{-}lacZ}$ (*GNZ*)[22] can therefore be used to label epithelial cells using tissue-specific Cre lines; in our hands, this specific nuclear reporter exhibited faster bleaching over the long time-course used in live imaging. Therefore, we utilized the membrane-GFP reporter (*ROSA26-mTmG*^{flox}) to follow epithelial cell movements in our studies. This required a method for identifying and tracing individual cells by a membrane signal. To solve this problem, we utilized a modified cell tracking method (**Figure 3 and Protocol section 4**).

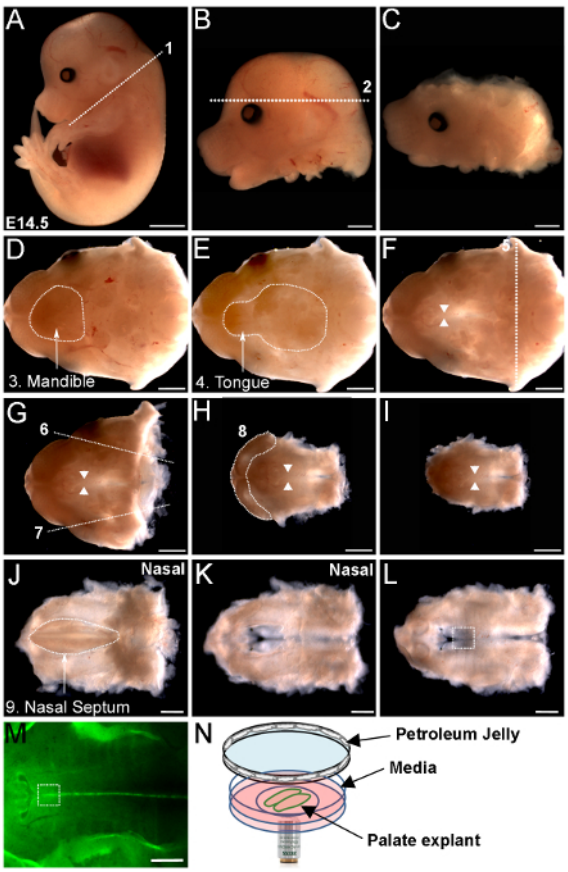

Figure 1: Schematic view of mouse secondary palate dissection. (**A**) Side view of E14.5 mouse embryo. To dissect palatal shelves, the head was cut along the first white dotted line, #1. (**B, C**) The upper brain (above the second white line, #2) was removed. (**D, E**) Oral view of dissected head. Lower mandible (#3) was dissected and tongue (#4) was removed. (**F**) Posterior part of the head along the line #5 was cut out. (**G-I**) Both maxillae (#6, #7) and anterior part of upper jaw (#8) were removed. (**J-L**) Nasal septum (#9) was removed (**M**) GFP signals in the MES of dissected palate from a *K14-cre; ROSA26*^{mTmG} mouse embryo. (**N**) Live imaging setup. The oral side of the palate explant was facing down to be imaged with inverted confocal microscope. MES is indicated with white arrowheads (**F-I**). The imaged area is indicated by white dotted boxes in L and M. Scale bars = 2 cm in A, 1 cm in B-I, 500 µm in J-M. Please click here to view a larger version of this figure.

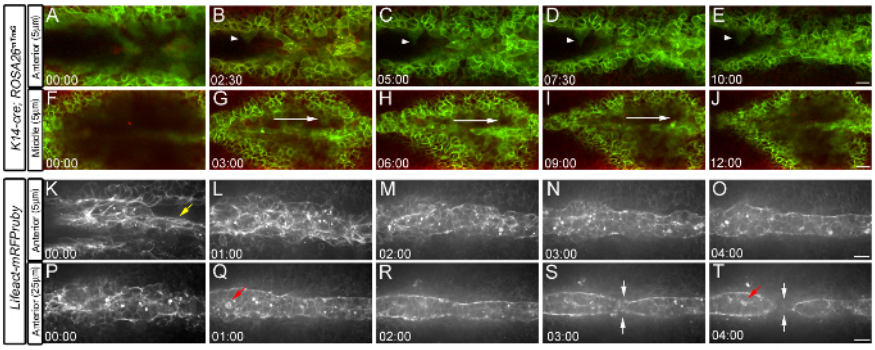

Figure 2: Live imaging of palate explant cultures. (**A-E**) Live imaging of the anterior secondary palate from a *K14-cre; ROSA26*^{mTmG} explant (5 μm depth). The white arrowhead shows a membrane protrusion from an epithelial cell (**F-J**) Live imaging of the middle palate from *K14-cre; ROSA26*^{mTmG} explant (5 μm depth). White arrows indicate the direction of cell migrations from the anterior to posterior palate. (**K-O**) Live imaging of the anterior palate from *Lifeact-mRFPruby* explant (5 μm depth). Epithelial cell displacement (yellow arrow) to the oral surface and convergence to form an integrated MES with cable-like actin structures in the midline. (**P-T**) Live imaging of the anterior palate from *Lifeact-mRFPruby* explant (25 μm depth). The red arrow indicates a cell extrusion event (**Q, T**). Future breakage points of the seam are indicated by two vertical white arrows in S and T. Scale bars = 20 μm. All live imaging data in this figure is derived from experiments previously published in[6]. Please click here to view a larger version of this figure.

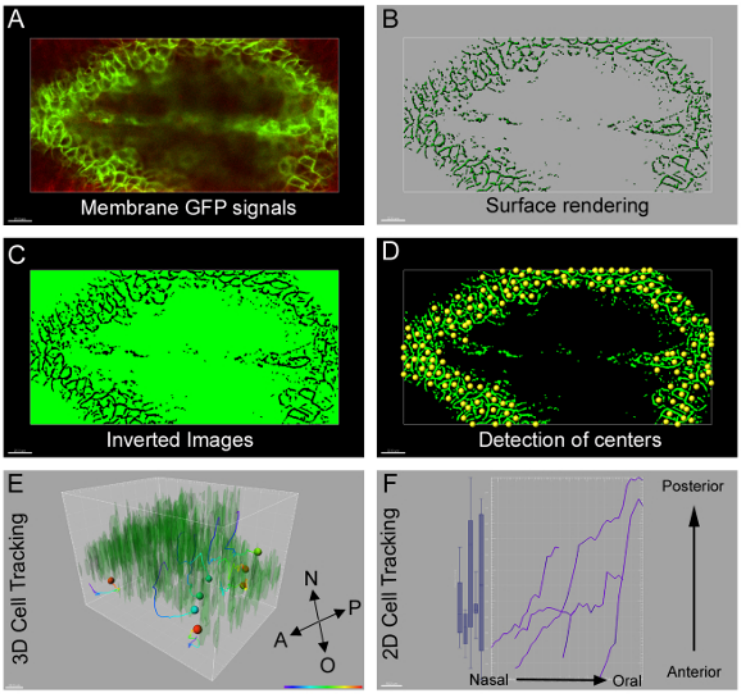

Figure 3: Data analysis. (**A-D**) To trace epithelial cells with membrane GFP signals from *K14-cre; ROSA26*^{mTmG} palate explant (**A**), A surface was generated by volume rendering of the membrane GFP signal (**B**). Inverted images were generated after masking the created surface (**C**). Cellular centers were identified from the inverted images using a spots detection function in Imaris (**D**). (**E**) 3D reconstructions allow tracking cell movements in multiple directions. A: anterior, P: posterior, N: nasal, O: oral (**F**) 2D analysis generates a vantage plot showing cells migrating from anterior to posterior direction in middle palate MES. Scale bars = 20 μm in A-D, 10 μm in E-F. Please click here to view a larger version of this figure.

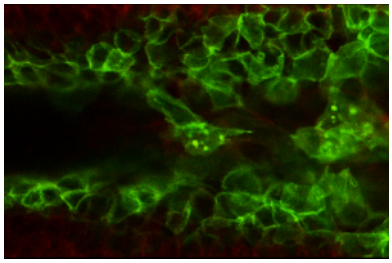

Video Figure 1: Live imaging of *K14-cre; ROSA26-mTmG*^{flox} anterior palate (5 µm depth). Images were captured every 10 min (10 min/frame) for 16 h 20 min, Scale bar = 25 µm. This video is a different Z-position of a movie previously published in reference[6]. Please click here to view this video. (Right-click to download.)

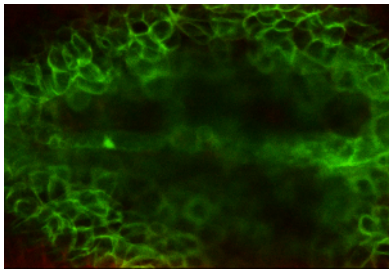

Video Figure 2: Live imaging of *K14-cre; ROSA26-mTmG*^{flox} middle palate (5 µm depth). Images were captured every 15 min (15 min/frame) for 13 h 30 min, Scale bar = 25 µm. This video has been previously published in reference[6]. Please click here to view this video. (Right-click to download.)

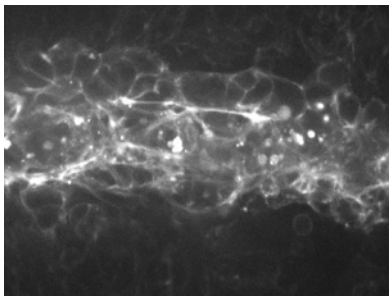

Video Figure 3: Live imaging of *Lifeact-mRFPruby* anterior palate (5 µm depth).
Images were taken every 10 min (10 min/frame) for 7 h 50 min. Scale bar = 20 µm. This video has been previously published in reference[6]. Please click here to view this video. (Right-click to download.)

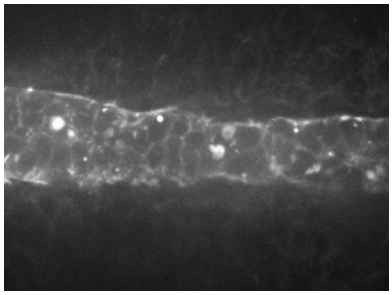

Video Figure 4: Live imaging of *Lifeact-mRFPruby* anterior palate (25 µm depth).
Images were taken every 10 min (10 min/frame) for 7 h 50 min. Scale bar = 20 µm. This video is a different Z-position of a movie previously published in reference[6]. Please click here to view this video. (Right-click to download.)

Discussion

Live imaging of tissue morphogenesis with 3D organ explant culture can provide detailed information regarding cellular processes that cannot be shown in conventional staining analysis of fixed tissue sections. Using *in vitro* explant culture of mouse embryonic secondary palate, we observed several interesting cellular behaviors leading us to propose a novel mechanism of palate fusion that involves epithelial convergence and cell extrusion.

One common challenge in studies of this type is photobleaching by continuous laser excitations over a long time-course. In our studies, a white light confocal and a spinning disk confocal microscope were used. Some decrease in signal intensity over time could be corrected by bleaching corrections in the imaging software (LAS-AF) (Protocol 4.1). Because bleaching correction is limited, it is important to carefully optimize laser

power and exposure time in each imaging system. We also checked that palate fusion occurs normally in the live imaging media after 3 day culture[6].

A second common issue in live imaging is tissue drift. It is critical to minimize drift to get consistent images during live imaging because changes in the focal plane can confound an understanding of morphogenetic changes over time. Whereas controlling thermal drift can be achieved in many confocal microscopes (Definite focus in the microscope), the drift of the tissue relative to the glass bottom cannot be corrected by these methods. Utilization of agarose, as well as placing the explant against the glass-bottom helps to minimize this, but care still must be taken only to analyze those movies that maintain a relatively constant position. This can be determined by following multiple control points in the imaging field across time to determine if they remain constant, move with a similar trend, or move differently. To an extent, using post-processing functions allow a correction of some tissue drift in live imaging (Protocol 4.2).

Low melting agarose was used at a final concentration of 0.6% in the live imaging media to immobilize the explant tissues. When we tested higher concentrations of agarose, they appeared to impair tissue morphogenesis possibly due to mechanical constraint. It is therefore important to use the correct agarose concentration to minimize tissue drift while not disturbing morphogenesis.

Due to confocal imaging depth, this method does pose limits in examining very deep Z planes of palate fusion. Using both the WHITE LIGHT and spinning disk confocal microscopes, signal from 100 µm depths could be imaged successfully though the image began to become dull and faint beyond this limit. Because palate fusion is a progressive process in the oronasal and anteroposterior axes, we propose that imaging multiple positions effectively allows imaging of different depths of palate fusion, but two-photon or light sheet confocal microscopy may be employed in the future to improve depth of imaging. In most of our experiments, the oral side of palate explants was imaged. Imaging of the nasal side of the palate explant is difficult because the nasal septum is fused or very close to the secondary palatal shelves. In our attempts to image fusion from the nasal side, it was also necessary to remove the extra nasal tissue so it did not interfere with the signal from the palate epithelium. Though possible, imaging the nasal side of the palate explant was difficult because dissection of the nasal septum often caused damage to the palate explants.

Live imaging of reporter mouse tissue explants is a powerful method to study cellular mechanisms of tissue morphogenesis during embryonic development. Using confocal microscopy techniques and quantitative imaging analysis, basic developmental processes such as secondary palate fusion can be investigated at the cellular level.

Disclosures

The authors have nothing to disclose.

Acknowledgements

We thank M. Douglas Benson for initial conversations regarding secondary palate imaging. We also acknowledge David Castaneda-Castellanos (Leica) and Chris Rieken (Zeiss) for their help to adjust imaging conditions in confocal microscopy. We appreciate Lynsey Hamilton (Bitplane) for helpful suggestions for quantitative image analysis using Imaris software. This work was funded by NIH/NIDCR R01 DE025887.

References

1. Ray, H. J., & Niswander, L. Mechanisms of tissue fusion during development. *Dev. Camb. Engl.* **139,** 1701-1711 (2012).
2. Dudas, M., Li, W.-Y., Kim, J., Yang, A., & Kaartinen, V. Palatal fusion - where do the midline cells go? A review on cleft palate, a major human birth defect. *Acta Histochem.* **109,** 1-14 (2007).
3. Bush, J. O., & Jiang, R. Palatogenesis: morphogenetic and molecular mechanisms of secondary palate development. *Development*. **139,** 231-243 (2012).
4. Lan, Y., Xu, J., & Jiang, R. Cellular and Molecular Mechanisms of Palatogenesis. *Curr Top Dev Biol*. **115,** 59-84 (2015).
5. Taya, Y., O'Kane, S., & Ferguson, M. W. Pathogenesis of cleft palate in TGF-b3 knockout mice. *Development*. **126,** 3869-3879 (1999).
6. Kim, S. *et al.* Convergence and Extrusion Are Required for Normal Fusion of the Mammalian Secondary Palate. *PLOS Biol.* **13,** e1002122 (2015).
7. Yoshida, M. *et al.* Periderm cells covering palatal shelves have tight junctions and their desquamation reduces the polarity of palatal shelf epithelial cells in palatogenesis. *Genes Cells*. **17,** 455-472 (2012).
8. Fitchett, J., & Hay, E. Medial edge epithelium transforms to mesenchyme after embryonic palatal shelves fuse. *Dev. Biol.* **131,** 455-474 (1989).
9. Akira, N. *et al.* The expression of TGF-beta3 for epithelial-mesenchyme transdifferentiated MEE in palatogenesis. *J Mol Hist*. **41,** 343-355 (2010).
10. Sani, F. V. *et al.* Fate-mapping of the epithelial seam during palatal fusion rules out epithelial-mesenchymal transformation. *Dev. Biol.* **285,** 490-495 (2005).
11. Jin, J.-Z., & Ding, J. Analysis of cell migration, transdifferentiation and apoptosis during mouse secondary palate fusion. *Development*. **133,** 3341-3347 (2006).
12. Xu, X. *et al.* Cell autonomous requirement for Tgfbr2 in the disappearance of medial edge epithelium during palatal fusion. *Dev. Biol.* **297,** 238-248 (2006).
13. Carette, M. J., & Ferguson, M. W. The fate of medial edge epithelial cells during palatal fusion in vitro: an analysis by DiI labelling and confocal microscopy. *Development.* **114,** 379-388 (1992).
14. Muzumdar, M., Tasic, B., Miyamichi, K., Li, L., & Luo, L. A global double-fluorescent Cre reporter mouse. *Genesis*. **45,** 593-605 (2007).
15. Dassule, H., Lewis, P., Bei, M., Mass, R., & McMahon, A. Sonic hedgehog regulates growth and morphogenesis of the tooth. *Development*. **127,** 4775-4785 (2000).
16. Eisenhoffer, G. *et al.* Crowding induces live cell extrusion to maintain homeostatic cell numbers in epithelia. *Nature*. **484,** 501-546 (2012).

17. Riedl, J. *et al.* Lifeact: a versatile marker to visualize F-actin. *Nat Methods*. **5,** 605-607 (2008).
18. Riedl, J. *et al.* Lifeact mice for studying F-actin dynamics. *Nat Methods.* **7,** 168-169 (2010).
19. Can, A. *et al*. Attenuation correction in confocal laser microscopes: a novel two-view approach. *J Microsc*. **211** (2003).
20. Veenman, C., Reinders, M., & Backer, E. Resolving motion correspondence for densely moving points. *IEEE Trans Pattern Anal Mach Intell*. **23,** 54-72 (2001).
21. Udan, R., Piazza, V., Hsu, C., Hadjantonakis, A., & Dickinson, M. Quantitative imaging of cell dynamics in mouse embryos using light-sheet microscopy. *Development.* **141,** 4406-4414 (2014).
22. Stoller, J. *et al.* Cre reporter mouse expressing a nuclear localized fusion of GFP and beta-galactosidase reveals new derivatives of Pax3-expressing precursors. *Genesis.* **46,** 200-204 (2008).

